Mechanism-Oriented Controllability of Intracellular Quantum Dots Formation: The Role of Glutathione Metabolic Pathway

Yong Li,[†] Ran Cui,[†] Peng Zhang,[‡] Bei-Bei Chen,[†] Zhi-Quan Tian,[†] Li Li,[†] Bin Hu,[†] Dai-Wen Pang,[†,*] and Zhi-Xiong Xie[‡,*]

[†]Key Laboratory of Analytical Chemistry for Biology and Medicine (Ministry of Education), College of Chemistry and Molecular Sciences, State Key Laboratory of Virology, and Wuhan Institute of Biotechnology, and [‡]College of Life Sciences, Wuhan University, Wuhan, 430072, P. R. China

ABSTRACT Microbial cells have shown a great potential to biosynthesize inorganic nanoparticles within their orderly regulated intracellular environment. However, very little is known about the mechanism of nanoparticle biosynthesis. Therefore, it is difficult to control intracellular synthesis through the manipulation of biological processes. Here, we present a mechanism-oriented strategy for controlling the biosynthesis of fluorescent CdSe quantum dots (QDs) by means of metabolic engineering in yeast cells. Using genetic techniques, we demonstrated that the glutathione metabolic pathway controls the intracellular CdSe QD formation. Inspired from this mechanism, the controllability of CdSe QD yield was realized through engineering the glutathione metabolism in genetically modified yeast cells. The yeast cells were homogeneously transformed into more efficient cell-factories at the single-cell level, providing a specific way to direct the cellular metabolism toward CdSe QD formation. This work could provide the foundation for the future development of nanomaterial biosynthesis.

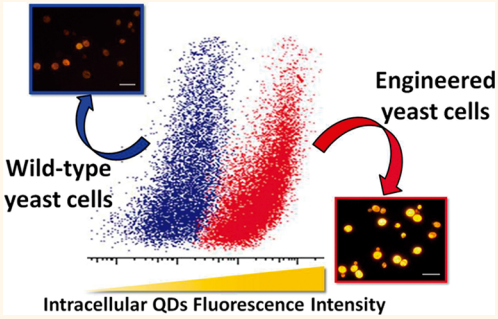

KEYWORDS: biosynthesis · quantum dots · mechanism · controllability · glutathione metabolic pathway · yeast

Nanomaterials with the unique properties[1−3] have wide applications in diagnosis,[4] biosensing,[5] catalysis,[6] and electro-optic devices.[7] These applications, particularly applications in biomedicine, require the proper design and synthesis of nanomaterials.[8] Conventional strategies used for the production of nanomaterials often involve toxic reagents, strong reducing agents, and high temperatures and pressures, which have been proven to be environmentally unfriendly, energy-inefficient, and difficult to control.[8] Currently, the use of biological systems to synthesize nanomaterials represents an under-explored but promising alternative for addressing these issues.[9−13] Many environmental organisms have developed the natural mechanisms to synthesize nanomaterials.[14−17] On the other hand, some model microorganisms could also be utilized for the synthesis of nanomaterials.[18−23] The rational coupling of the intrinsic biochemical pathways in the model microorganism allows for the precise and efficient production of nanomaterials.[18]

The biosynthesis of nanomaterials occurs within the mild and highly organized cellular environment. The distinct aspects of the intracellular synthesis of nanomaterials, such as the preparation of precursors, the formation of nanocrystals, and the encapsulation of final products, are dictated by the expression of specific genes.[24,25] These synthesis-specific genes are further integrated through the complex networks of cellular metabolism and regulation. Therefore, the controllability of nanomaterial biosynthesis is coupled with the concerted actions of different biological processes in time and space.[18] Understanding how these biological processes contribute to the formation of nanomaterials will enable further design of biosynthetic pathways for the optimal production of nanomaterials. The main challenge of such efforts is to reliably and conveniently define the role of a given gene and metabolic pathway in nanomaterial formation.

* Address correspondence to dwpang@whu.edu.cn, zxxie@whu.edu.cn.

Received for review November 18, 2012 and accepted February 9, 2013.

Published online February 09, 2013
10.1021/nn305346a

In our previous work, the budding yeast *Saccharomyces cerevisiae* was employed as a biosynthesizer to manufacture fluorescent CdSe quantum dots (QDs).[18] By temporally and spatially coupling the intracellular irrelated biochemical reactions, this strategy realized the controllable biosynthesis of CdSe QDs in a model microorganism, which is different from the naturally evolved nanomaterial formation in the environmental organisms. The intracellular routes for CdSe QDs have also been applied to direct the *in vitro* synthesis of size-tunable gold nanoparticles,[26] Au−Ag alloy nanoparticles,[27] gold clusters,[28] PdSe nanocubes,[29] and near-infrared Ag_2Se QDs.[30] Therefore, exploring the mechanism of intracellular CdSe QD formation will be informative for further engineering microorganism toward nanomaterial syntheses, and it will expand our view of the fundamental relationship between biological processes and the formation of inorganic materials at the nanoscale.

Herein, using genetic techniques and CdSe QD fluorescence as an intracellular indicator, we explored the biosynthetic mechanism of CdSe QDs in living yeast cells. We found that the glutathione metabolic pathway is important for the biosynthetic yield of CdSe QDs. Further evidence showed that the intracellular formation of CdSe QDs is tightly controlled by the expression of the glutathione metabolic gene. Inspired from this intrinsic mechanism, the glutathione metabolic pathway was engineered to improve the biosynthetic yield of CdSe QDs in genetically modified yeast cells. In this mechanism-oriented strategy, the key gene required for the biosynthesis of CdSe QDs was specifically modified, and the yeast cells were homogeneously transformed into more efficient cell-factories at the single-cell level.

RESULTS AND DISCUSSION

The role of Glutathione Metabolism in the Biosynthesis of CdSe QDs. It is important to identify the key biomolecules and metabolic pathways involved in the intracellular synthesis of nanomaterials. As a ubiquitous tripeptide, glutathione (L-γ-glutamylcysteinylglycine) possesses a unique γ-glutamylcysteine peptide bond and thiol group. These features mediate the cellular metabolism of inorganic compounds,[31,32] and can be used to inspire *in vitro* synthesis of QDs.[29,30] However, the intracellular correlation between glutathione metabolism and QD formation remains unclear and somewhat controversial.[19,33]

We used the gene deletion technique to explore the role of glutathione metabolism in the biosynthesis of CdSe QDs. This technique allowed us to determine gene functions by completely and specifically removing such a gene from wild-type (WT) cells.[34,35] In yeast, the *GSH1* gene encodes γ-glutamylcysteine ligase (GCL), which catalyzes the first and rate-limiting reaction of cellular glutathione synthesis (Scheme 1).[36] Deletion of *GSH1* gene generates the Δ*gsh1* mutant strain, which is unable to produce glutathione.[36] To determine whether the glutathione metabolic pathway is involved in the intracellular synthesis of CdSe QDs, we compared the ability of WT and Δ*gsh1* mutant cells to biosynthesize CdSe QDs.

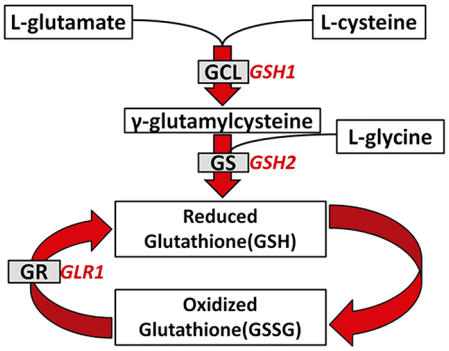

Scheme 1. Glutathione metabolic pathway in yeast cells. The first and rate-limiting reaction of cellular glutathione synthesis is the formation of dipeptide γ-glutamylcysteine, which is catalyzed by the *GSH1*-encoded γ-glutamylcysteine ligase (GCL). The γ-glutamylcysteine is further reacted with the glycine to produce glutathione, which is catalyzed by the *GSH2*-encoded glutathione synthetase (GS). The *GLR1* gene encodes glutathione reductase (GR), which catalyzes the reduction of oxidized glutathione (GSSG) to reduced glutathione (GSH).

By using the previously established method,[18] the WT yeast cells showed strong intracellular fluorescence (Supporting Information, Figure S1). The isolated fluorescent materials were well-dispersed nanoparticles, which had lattice spacings of 0.21 and 0.18 nm, corresponding to the (111) and (201) facets of CdSe (Supporting Information, Figure S2). The photoluminescence (PL) emission peak of isolated CdSe QDs was at 575 nm with good photostability and quantum yield of 4.7% (Supporting Information, Figure S3). These results suggested that the fluorescence of biosynthesized CdSe QDs can be used as a visual and intracellular indicator to testing mutant strains. Compared with the WT cells, Δ*gsh1* mutant cells exhibited a significantly lower fluorescence intensity of intracellular CdSe QDs (Figure 1). Owing to the complete loss of glutathione synthesis in Δ*gsh1* mutants, these results suggested that the glutathione metabolic pathway is important for the biosynthesis of CdSe QDs.

The *GSH2* gene encodes glutathione synthetase (GS), which catalyzes the second reaction of glutathione synthesis (Scheme 1).[37] Cells harboring a deletion of the *GSH2* gene (Δ*gsh2* mutant strain) cannot produce glutathione, but they accumulate dipeptide γ-glutamylcysteine.[37] As an intermediate in the glutathione metabolic pathway, the γ-glutamylcysteine has nearly all of the features of glutathione, including a γ-glutamylcysteine peptide bond and a thiol group. However, deletion of the *GSH2* gene also led to a significant decrease in the intracellular CdSe QD fluorescence intensity (Figure 1).

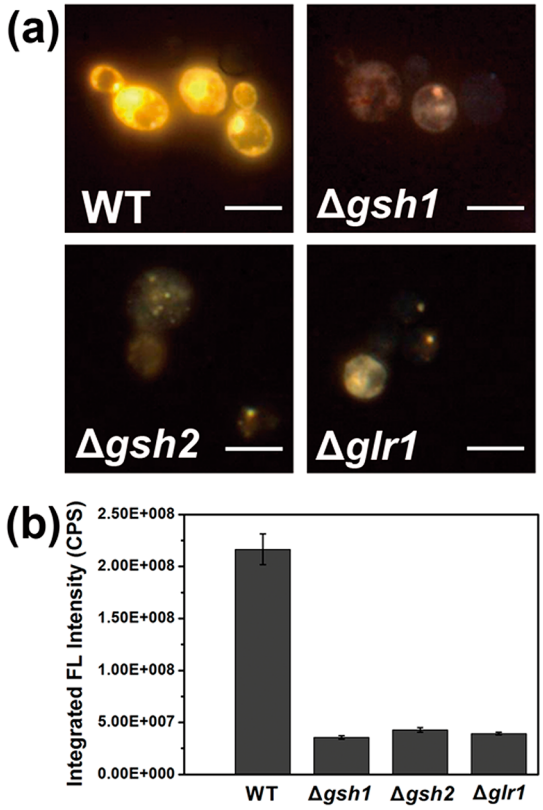

Figure 1. Fluorescence microscopic images (a) and the intracellular CdSe QD fluorescence intensity (b) of the WT, Δ*gsh1*, Δ*gsh2*, and Δ*glr1* cells. Exposure time, 200 ms; scale bar, 5 μm.

This result indicated that the γ-glutamylcysteine cannot act as a substitute for the role of glutathione in the biosynthesis of CdSe QDs. Therefore, the naturally evolved structure and composition of glutathione are crucial for the biosynthesis of CdSe QDs.

To determine the effect of deleting both the *GSH1* and *GSH2* genes on the biosynthesis of CdSe QDs, a Δ*gsh1*Δ*gsh2* double mutant strain was constructed (Supporting Information, Figure S4). The intracellular CdSe QD fluorescence intensity of Δ*gsh1*Δ*gsh2* cells was similar to those of Δ*gsh1* and Δ*gsh2* cells (Supporting Information, Figure S5), indicating that the double deletion of the *GSH1* and *GSH2* genes did not have more significant effect on the biosynthesis of CdSe QDs. This could be attributed to the fact that the glutathione synthesis is a serial but not a parallel process.[36,37]

Oxidized glutathione (GSSG) is another cellular metabolic form of glutathione (Scheme 1). The existence of *GLR1* gene maintains the high ratio of reduced-to-oxidized glutathione in yeast cells.[38] Deletion of this gene leads to the accumulation of high levels of GSSG in Δ*glr1* mutant cells.[38] Thus, the Δ*glr1* mutant strain was used to test the role of glutathione redox state in the biosynthesis of CdSe QDs. We found that the Δ*glr1* mutant cells also exhibited the decreased intracellular CdSe QD fluorescence intensity (Figure 1), suggesting that the redox state of glutathione is an important factor for the biosynthesis of CdSe QDs.

As previously reported,[18,19] the biosynthesis of QDs is also correlated with the cell growth phase. The growth curves of the WT and glutathione metabolic mutant strains tested above were analyzed by measuring the optical density at 600 nm (Supporting Information, Figure S6). All of the strains entered the stationary phase after 24 h of culturing. However, the Δ*gsh1* and Δ*gsh1*Δ*gsh2* strains showed a decreased cell density in the stationary phase. These results were consistent with the role of *GSH1* gene in the cell growth.[39]

To examine the effect of growth phase on the biosynthesis of CdSe QDs, the cultures of all strains in the exponential and stationary phase were adjusted to the same cell density (OD_{600} = 12) before biosynthesis. For each strain, the stationary phase cells showed a much stronger intracellular CdSe QD fluorescence intensity than the exponential phase cells (Supporting Information, Figure S7). These results indicated that the stationary phase cells have a greater capability to biosynthesize CdSe QDs, and were consistent with the previous reports on QD biosynthesis.[18,19] This is probably explained by the enhanced ability of stationary phase cells to respond to cadmium and selenite.[40,41] Furthermore, compared with the WT strain, glutathione metabolic mutant strains showed a significantly decreased intracellular CdSe QD fluorescence intensity in all growth phases (Supporting Information, Figure S7). These results suggested the important role of glutathione metabolic pathway in the biosynthesis of CdSe QDs.

To further investigate the mechanism of intracellular CdSe QD formation, the biosynthesized CdSe QDs were isolated from the WT and glutathione metabolic mutant strains. The first excitonic absorption peak intensity of CdSe QDs isolated from the mutant cells was lower than that of CdSe QDs isolated from WT cells (Figure 2a). Because the first excitonic absorption peak intensity reflects the contents of QDs in a given sample,[42] our measured values were used to evaluate the biosynthetic yield of CdSe QDs. As shown in Figure 2b and Supporting Information, Table S1, deletion of the *GSH1*, *GSH2*, and *GLR1* genes led to the significant reduction of CdSe QD yield. These results were consistent with the decreased CdSe QD fluorescence intensity in the glutathione metabolic mutant cells, and suggested that the biosynthetic yield of CdSe QDs is controlled by the glutathione metabolic pathway.

Glutathione-Based Control of Intracellular CdSe QD Formation. As previously reported,[18] there are two steps that are coupled in the biosynthetic procedures of CdSe QDs: The first step is the cellular reduction of Na_2SeO_3 leading to the accumulation of selenocystine, which is the precursor for CdSe QDs; the second step is the treatment of seleniumized yeast cells with $CdCl_2$, which

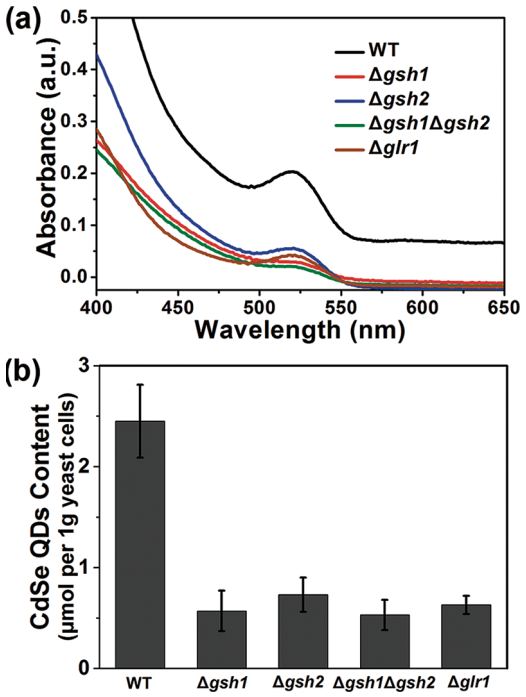

Figure 2. Measurement of CdSe QD yields in the WT and glutathione metabolic mutant cells. (a) UV−vis spectra of CdSe QDs isolated from the WT, Δ*gsh1*, Δ*gsh2*, Δ*gsh1*Δ*gsh2*, and Δ*glr1* cells. (b) Biosynthetic yield of CdSe QDs in the WT, Δ*gsh1*, Δ*gsh2*, Δ*gsh1*Δ*gsh2*, and Δ*glr1* cells.

initiates the formation of CdSe QDs. This raised the question of whether glutathione metabolism has an effect on the intracellular preparation of selenocystine precursor, or whether it plays a direct role in the intracellular formation of CdSe QDs during the cadmium treatment. The Δ*gsh1* strain was used to address this question because of the inability of this strain to synthesize glutathione.[36] High-performance liquid chromatography coupled with inductively coupled plasma mass spectrometry (HPLC−ICP−MS) measurements showed that the major intracellular low-valence selenium[43] could be well separated and detected in our experiments (Figures 3a−c). By comparing the HPLC−ICP−MS results obtained from the seleniumized WT and Δ*gsh1* cells, we found that the deletion of the *GSH1* gene causes a moderate decrease in the intracellular contents of selenocystine precursor (Figures 3b,c). This result indicated that glutathione metabolism only has a limited effect on the intracellular preparation of the selenocystine precursor.

It should be noted that although the glutathione metabolic pathway does not play a central role in the intracellular preparation of the selenocystine precursor, its contribution to the biosynthesis of CdSe QDs is still significant. This implies that the importance of the glutathione metabolic pathway is mainly reflected in the process of CdSe QD formation after the addition of $CdCl_2$. To confirm this hypothesis, the seleniumized Δ*gsh1* mutant cells were incubated with either $CdCl_2$ alone or $CdCl_2$ plus 1 mM reduced glutathione. As

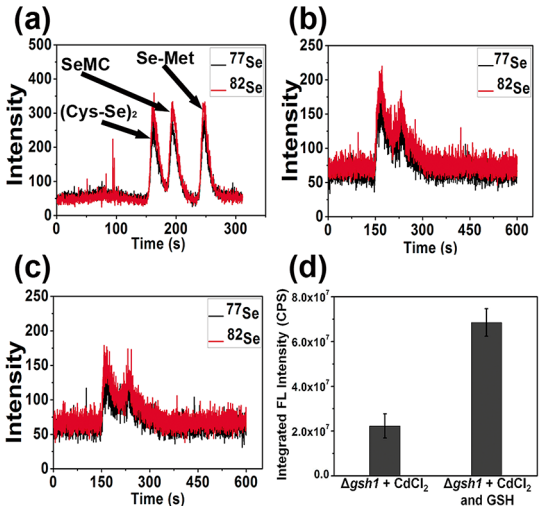

Figure 3. HPLC−ICP−MS chromatograms of selenium species standards (a) and selenoamino acids isolated from the seleniumized WT (b) and Δ*gsh1* (c) cells. The selenium species standards are: L-selenocystine $(Cys\text{-}Se)_2$, Se-methyl-seleno-L-cysteine (SeMC), and D,L-selenomethionine (Se-Met). (d) Intracellular CdSe QD fluorescence intensity of seleniumized Δ*gsh1* mutant cells incubated with either $CdCl_2$ alone or $CdCl_2$ plus 1 mM reduced glutathione (GSH).

shown in Figure 3d, the ability of Δ*gsh1* cells to biosynthesize CdSe QDs was partially recovered as a result of the addition of exogenous glutathione during the cadmium treatment. This result indicated that glutathione and its metabolic pathway plays a direct role in the intracellular formation of CdSe QDs.

In a cell, nearly all of the biological processes are dictated by the gene expression patterns.[44] To understand how cells control CdSe QD formation, the expression of glutathione metabolic genes was analyzed by the real-time reverse transcription polymerase chain reaction (qRT-PCR). The transcription levels of the *GSH1*, *GSH2*, and *GLR1* genes in the seleniumized yeast cells were similar to those in normal yeast cells (Figure 4a), which was consistent with the limited effect of glutathione metabolism on the intracellular preparation of the selenocystine precursor. However, exposure of seleniumized yeast cells to $CdCl_2$ resulted in an 8-fold increase in the expression of the *GSH1* gene (Figure 4a). It has been previously reported that *GSH1*-encoded GCL catalyzes the rate-limiting reaction in the cellular glutathione synthesis.[36] The regulation of *GSH1* expression is vital for modulation of cellular glutathione contents. Therefore, the enhanced *GSH1* expression observed here indicated that there is an increased glutathione requirement during intracellular CdSe QD formation.

Despite the significant effect of the *GSH2* and *GLR1* genes on the biosynthesis of CdSe QDs, the expression of the two genes was not up-regulated dramatically in the presence of cadmium (Figure 4a). This observation can be explained by the fact that intracellular glutathione contents are tightly regulated by the rate-limiting role of the *GSH1* gene. Furthermore, the

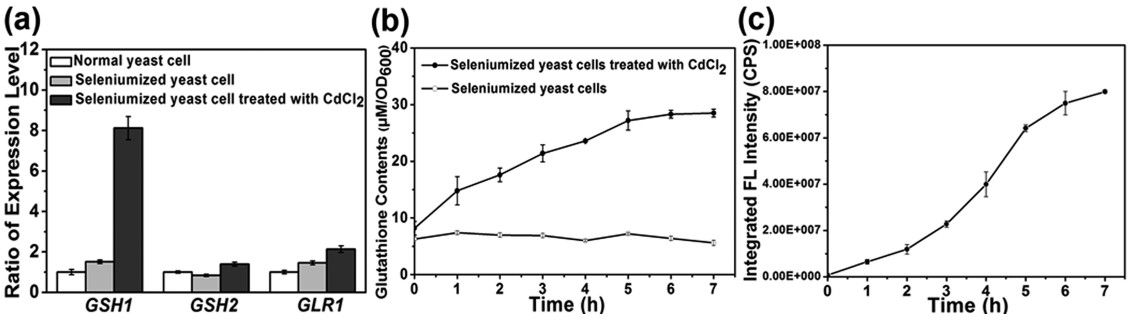

Figure 4. The expression levels of glutathione metabolic genes and intracellular glutathione contents of yeast cells. (a) Expression levels of the *GSH1*, *GSH2*, and *GLR1* genes. The expression levels of the different samples were normalized to normal yeast cells that were not treated with Na_2SeO_3 and $CdCl_2$. (b) Intracellular glutathione contents of seleniumized yeast cells and seleniumized yeast cells treated with $CdCl_2$. (c) Intracellular CdSe QD fluorescence intensity of the seleniumized yeast cells during $CdCl_2$ treatment.

up-regulation of the rate-limiting *GSH1* gene as opposed to other glutathione metabolic genes suggested a precise and economic way for yeast cells to control CdSe QD formation.

We further investigated the correlation between cellular glutathione contents and CdSe QD formation. Figures 4b,c showed a synchronized increase in the contents of intracellular glutathione and fluorescence intensity of CdSe QDs during initial cadmium incubation, suggesting that the CdSe QD formation was synergistic with the intracellular regulation of the glutathione contents. Together, our results demonstrated a mechanism for the glutathione-based control of CdSe QD formation, in which the rate-limiting *GSH1* gene was up-regulated to meet the increased requirement of glutathione contents during the intracellular formation of CdSe QDs. This intrinsic mechanism could provide a guideline for optimization of intracellular CdSe QD synthesis.

Mechanism-Oriented Controllability of Intracellular CdSe QD Synthesis. A challenge in the biosynthesis of nanomaterials is to rationally control the intracellular synthetic processes. Inspired from the mechanism characterized above, we further attempted to control the intracellular CdSe QD formation by engineering the glutathione metabolic pathway. To accomplish this, the P_{GAL1}-*GSH1*, P_{GAL1}-*GSH2*, and P_{GAL1}-*GLR1* strains were constructed using standard genetic techniques (Figure 5a and Supporting Information, Figure S8).[35] In these strains, the expression of genetically modified *GSH1*, *GSH2*, and *GLR1* genes could be induced by galactose respectively.

The growth curves of the WT and the genetically modified strains were analyzed under galactose-induced conditions (Supporting Information, Figure S9). Compared with the WT strain, the genetically modified strains showed a slower growth rate in the exponential phase. However, in the stationary phase, the cell density of the genetically modified strains was not affected by the genetic manipulation. Because the biosynthesis of CdSe QDs was performed in the stationary phase, our results suggested that these genetically modified

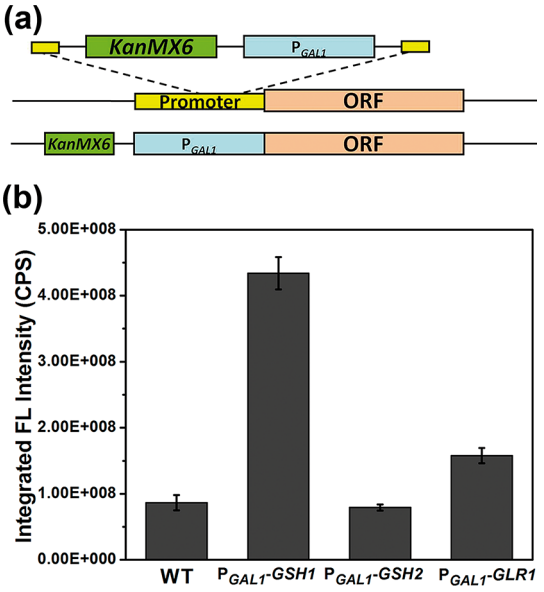

Figure 5. (a) Strategy for the construction of genetically modified strains. PCR products containing the galactose-inducible P_{GAL1} promoter and the *KanMX6* selectable marker were inserted at the upstream of the open reading frame (ORF) of the *GSH1*, *GSH2*, and *GLR1* genes, yielding P_{GAL1}-*GSH1*, P_{GAL1}-*GSH2*, and P_{GAL1}-*GLR1* strains. (b) Intracellular CdSe QD fluorescence intensity of the WT, P_{GAL1}-*GSH1*, P_{GAL1}-*GSH2*, and P_{GAL1}-*GLR1* cells under galactose-induced conditions.

strains are good candidates for exploring the controllability of intracellular CdSe QD formation.

As described above, the intracellular glutathione contents are crucial for CdSe QD formation. Induction of the *GSH1* gene significantly increased the glutathione contents in the P_{GAL1}-*GSH1* cells (Supporting Information, Figure S10). Consistently, the P_{GAL1}-*GSH1* cells indeed exhibited a 5-fold higher intracellular CdSe QD fluorescence intensity than the WT cells under galactose-induced conditions (Figure 5b). Moreover, the P_{GAL1}-*GSH1* cells had a greater ability to biosynthesize CdSe QDs in the stationary phase (Supporting Information, Figure S11). Transmission electron microscopy (TEM) and high resolution TEM (HRTEM) measurements confirmed that the crystal structure of P_{GAL1}-*GSH1*

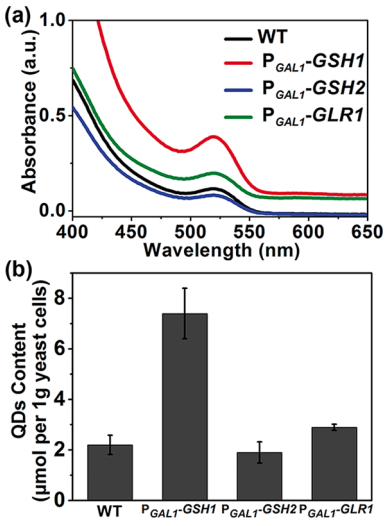

Figure 6. Measurement of the CdSe QD yields in the WT and genetically modified strains. (a) UV−vis spectra of CdSe QDs isolated from the WT, P_{GAL1}-*GSH1*, P_{GAL1}-*GSH2*, and P_{GAL1}-*GLR1* cells. (b) Biosynthetic yield of CdSe QDs in the WT, P_{GAL1}-*GSH1*, P_{GAL1}-*GSH2*, and P_{GAL1}-*GLR1* cells under galactose-induced conditions.

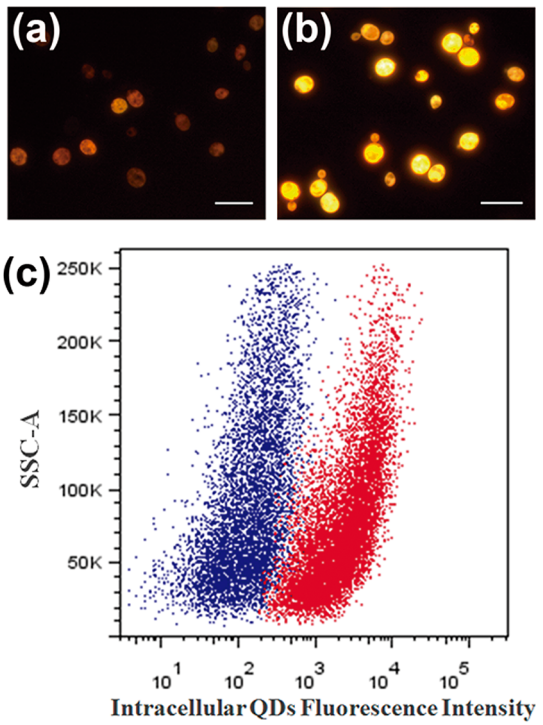

Figure 7. Fluorescence microscopic images of WT (a) and P_{GAL1}-*GSH1* (b) cells after biosynthesis of CdSe QDs: exposure time, 100 ms; scale bar, 10 μm. (c) Flow cytometry measurement of CdSe QD fluorescence intensity in the individual P_{GAL1}-*GSH1* (red) and WT (blue) cells. The nearly complete separation of the two cell populations emphasized the improved ability of the single P_{GAL1}-*GSH1* cells to biosynthesize CdSe QDs.

synthesized CdSe QDs is consistent with previously reported structures (Supporting Information, Figure S12a,b).[45] Further characterization showed that the PL emission peak of these CdSe QDs was at 575 nm (Supporting Information, Figure S12c). The first excitonic absorption intensity of CdSe QDs isolated from P_{GAL1}-*GSH1* cells was stronger than that of the corresponding CdSe QDs isolated from WT cells (Figure 6a). Therefore, the genetic modification of the rate-limiting *GSH1* gene improved the biosynthetic yield of CdSe QDs in the P_{GAL1}-*GSH1* strain (Figure 6b and Supporting Information, Table S1). These results indicated that the controllability of the biosynthetic yield of CdSe QDs was successfully realized by engineering the glutathione metabolic pathway.

However, the intracellular CdSe QD fluorescence intensity of the P_{GAL1}-*GSH2* and P_{GAL1}-*GLR1* cells was similar to that of the WT strain (Figure 5b and Supporting Information, Figure S11). Meanwhile, the biosynthetic yield of CdSe QDs in the P_{GAL1}-*GSH2* and P_{GAL1}-*GLR1* cells was not significantly improved (Figure 6 and Supporting Information, Table S1). These results indicated that genetic modification of the *GSH2* and *GLR1* genes has a limited effect on the biosynthesis of CdSe QDs. This result is reasonable because the induction of the *GSH2* and *GLR1* genes did not increase the glutathione contents in the P_{GAL1}-*GSH2* and P_{GAL1}-*GLR1* cells (Supporting Information, Figure S10). These results were consistent with the notion that the intracellular CdSe QD formation is tightly controlled by the expression of rate-limiting *GSH1* gene.

Because the P_{GAL1}-*GSH1* strain had an improved ability to biosynthesize CdSe QDs, we further examined the individual homogeneity of this strain. The CdSe QD fluorescence intensity of the individual P_{GAL1}-*GSH1* cells was much stronger than that of WT cells (Figures 7a,b). This observation was further confirmed by the flow cytometry measurements, which can quantitatively record the fluorescent signals from single cells. Figure 7c showed that nearly all of the P_{GAL1}-*GSH1* cells (95.5%) can be well distinguished from the WT cells through measuring the CdSe QD fluorescence intensity in the single cells. These results suggested that the improved ability of P_{GAL1}-*GSH1* to biosynthesize CdSe QDs could be attributed to the homogeneously engineered yeast cells.

Our results presented a mechanism-oriented strategy for the controllable biosynthesis of CdSe QDs in the genetically modified P_{GAL1}-*GSH1* strain. As a result, the yeast cells were homogeneously transformed into more efficient cell-factories at the single-cell level. This mechanism-oriented strategy could provide a specific way to direct the cellular metabolism toward the biosynthesis of CdSe QDs. In view of the recent progresses in the intracellular synthesis of nanomaterials,[21,22] the homogeneously engineered P_{GAL1}-*GSH1* strain may be a valuable tool for some fundamental applications, such as synthetic biology and cell-based sensors.[46,47]

CONCLUSION

In summary, we have demonstrated the important role of glutathione metabolic pathway in the biosynthesis

of CdSe QDs. Compared with the WT strain, the glutathione metabolic mutant strains showed significantly decreased fluorescence intensity and biosynthetic yield of CdSe QDs. This provides a genetic support for the important role of the glutathione metabolic pathway in the biosynthesis of CdSe QDs. Several lines of evidence strongly suggest that the intracellular formation of CdSe QDs is stringently controlled by the glutathione metabolic pathway. First, the glutathione plays a direct role in the biosynthesis of CdSe QDs. Second, the expression of rate-limiting *GSH1* gene is up-regulated to meet the increased requirement for glutathione during CdSe QD formation. Third, the CdSe QD formation is synergistic with the intracellular regulation of glutathione contents. Inspired from these findings, the biosynthetic yield of CdSe QDs has been improved in the homogeneously engineered P_{GAL1}-*GSH1* cells, providing a specific way to direct the cellular metabolism toward CdSe QD formation. This work will facilitate the future development of QD biosynthesis, as well as the design of quasi-biological systems,[26−30] which have applied the principle of temporally and spatially coupling the intracellular irrelated biochemical reactions to the *in vitro* synthesis of nanomaterials.

EXPERIMENTAL SECTION

Yeast Strains and Growth Conditions. All *Saccharomyces cerevisiae* strains used in this study were derived from the WT BY4742 strain (*MATα his3-Δ1 leu2-Δ0 lys2-Δ0 ura3-Δ0*). The Δ*gsh1*, Δ*gsh2*, and Δ*glr1* single mutant strains were obtained from the *Saccharomyces* Genome Deletion Project.[34] The Δ*gsh1*-Δ*gsh2*, P_{GAL1}-*GSH1*, P_{GAL1}-*GSH2*, and P_{GAL1}-*GLR1* strains were constructed in this study (for details, see Supporting Information). YP (1 g/L yeast extract and 2 g/L peptone) was supplemented with 2 g/L glucose or galactose to produce YPD or YPGal medium, respectively. Cultures of yeast with a volume no more than 20% of the vessel maximum were shaken at 200 rpm and 30 °C.

Biosynthesis of CdSe QDs. The biosynthesis of CdSe QDs was performed according to our previously described "time-space coupling" strategy.[18] Briefly, the stationary phase cells were first coincubated with 5 mM Na_2SeO_3 for 24 h to accumulate intracellular selenocystine precursors, and then the seleniumized yeast cells were harvested by centrifugation for 2 min at 3000*g*. The resulting cell pellets were resuspended in an equal volume of fresh YPD medium, and coincubated with 1 mM $CdCl_2$ to synthesize the CdSe QDs.

To examine the effect of the growth phase on the biosynthesis of CdSe QDs, cultures of all strains in the exponential and stationary phase (after 10 and 24 h of growth, respectively) were adjusted to the same cell density (OD_{600} = 12). The resulting cultures were used for the biosynthesis of CdSe QDs as described above.

For the induction of the P_{GAL1}-*GSH1*, P_{GAL1}-*GSH2*, and P_{GAL1}-*GLR1* strains, the WT and the three genetically modified strains were cultured in YPGal rather than YPD medium to induce gene expression during cadmium incubation.

Fluorescence Microscopy and Measurement of the Intracellular CdSe QD Fluorescence Intensity. Fluorescence micrographs were captured using an Olympus 1 × 51 inverted fluorescence microscope equipped with U-MWU filters (330−385/400/420 nm). The fluorescence spectra of the fluorescing and seleniumized cells (as cellular autofluorescence reference) were acquired using a Fluorolog-3 spectrometer (HORIBA Jobin Yvon France). The fluorescence intensity of intracellular CdSe QDs was calculated by subtraction of the cellular autofluorescence from the total intracellular fluorescence intensity of the fluorescing yeast cells. For the intracellular fluorescence intensity measurements and fluorescence microscopy imaging, all samples were washed and adjusted to a cell density of 6×10^7 cells mL^{-1} in 1 × phosphate buffered saline (PBS).

Purification and Characterization of Biosynthesized CdSe QDs. For the separation of intracellular synthesized CdSe QDs, 2 g (wet weight) of yeast cells were resuspended in 6 mL of lysis buffer (10 mM Tris-Cl pH 7.5, 0.2% sodium dodecyl sulfate (SDS)), and then disrupted with glass beads for six times of 1 min in a Mini-Bead Beater (Biospec USA) with 2-min breaks between the runs. Unbroken cells and cell debris were removed by centrifugation (10 min, 16 000*g*). The fluorescent supernatant was concentrated using an Amicon Ultra-15 100K Centrifugal Filter device. The resulting sample was loaded onto the top of a four-step sucrose gradient (3 mL, 60%; 2 mL, 45%; 2 mL, 30%; 2 mL, 8%), and centrifuged for 4 h at 134 000*g* and 4 °C. After centrifugation, the sucrose was removed by the gel electrophoresis and dialysis. The purified samples were washed three times by an Amicon Ultra-15 100K Centrifugal Filter device, and used for subsequent analysis. All of the buffers used for CdSe QDs isolation contained 1 × protease inhibitor cocktails. For transmission electron microscopy (TEM) and high resolution TEM (HRTEM) characterization, the purified CdSe QDs were diluted by 30-fold and dropped onto an ultrathin carbon-coated copper grid. The TEM images were taken on a Tecnai G2 20 S-TWIN transmission electron microscope at 200 kV, and the HRTEM images were taken on a JEOL-JEM 2010EF transmission electron microscope at 200 kV.

Determination of the CdSe QD Biosynthetic Yield. To determine the yield of CdSe QDs for the yeast strains used in this study, the total protein concentrations in all purified CdSe QDs samples were used as an internal control. Before the analysis, the total protein concentrations of each sample were measured using bicinchoninic acid (BCA) methods[48] and adjusted to 0.5 mg/mL in all samples. The UV−vis spectra of the adjusted samples were recorded on a Shimadzu UV-2550 UV−vis spectrophotometer. The obtained first excitonic absorption intensity of each sample was used to calculate the CdSe QD yield according to previously reported method.[42]

HPLC−ICP−MS. After treatment with Na_2SeO_3, approximately 1 g (wet weight) of WT or Δ*gsh1* mutant cells were harvested and washed three times with 1 × PBS by centrifugation (2 min, 3000*g*). The cell pellets were resuspended in the same buffer and disrupted in a Mini-Bead Beater (Biospec, USA) for 1 min. The resultant lysates were further treated with 200 mg of Trypsin in TCS buffer (0.1 M Tris-Cl pH 7.5, 10 mM $CaCl_2$, 0.5% SDS) for 18 h at 37 °C and then centrifuged at 10 000*g* for 10 min. The supernatant was filtered through a 0.22 μm filter and used for HPLC−ICP−MS measurement. The measurements were performed on an Agilent 7500 ICP-MS (Agilent, USA) coupled with an HPLC system (Shimadzu, Japan). The undigested proteins contained in samples were first removed by size-exclusion chromatography using a Superdex 200 HR 10/30 column (GE Healthcare USA). The selenoamino acids were separated using a CAPCELL PAK C18 column (Shiseido Japan) and detected online by ICP−MS.

RNA Isolation and qRT-PCR. The yeast total RNA was isolated according to the hot SDS/phenol extraction method.[49] The purified RNA was treated with DNase I to effectively remove traces of genomic DNA. The synthesis of the first-strand cDNA was performed with AMV reverse transcriptase and random primers following the manufacturer's recommendations. A sample of 25 ng of cDNA was used as a template for qPCR on a Stratagene MX3000P (Stratagene, USA) using Platinum SYBR Green qPCR kit and gene-specific primers (Supporting Information, Table S2). Each assay included a standard curve of five serial dilution points of cDNA, a no-template control, an RNA-template control, and 25 ng of each cDNA as template. The cycling program comprised initial incubations at 50 and 95 °C

and 40 cycles of 30 s at 95 °C, 30 s at 55 °C, and 30 s at 72 °C. After each run, a melting curve analysis was performed to ensure that no primer dimers were formed. The three internal control genes (*ACT1*, *IPP1*, and *PDA1*) were selected using the methods described by Vandesompele *et al.*[50] The expression levels of the tested genes in each sample were calculated and normalized to the selected internal control genes.

Measurement of Intracellular Glutathione. For measurement of the intracellular reduced glutathione, the cells were harvested and washed twice with ice-cold 1 × PBS by centrifugation for 2 min at 3 000*g*. The cell pellets were resuspended in the 1.3% (wt/vol) of ice-cold 5-sulfosalicylic acid and broken with glass beads in a Mini-Bead Beater for 1 min. The lysates was clarified by centrifugation for 10 min at 12 000*g*. The resulting supernatant was used to determine the total reduced glutathione contents according to the microtiter-based method described previously.[51] The glutathione contents are expressed as micromoles per OD_{600}, where one OD_{600} corresponds to a cell density of 2.5×10^7 cells mL^{-1}.

Flow Cytometry Measurement. The flow cytometry measurements were performed on a BD FACSAria flow cytometer (BD Biosciences, USA). The raw data were analyzed using FlowJo software. Before the measurements, the WT and P_{GAL1}-*GSH1* cells were washed and adjusted to 1×10^5 cells mL^{-1} in 1 × PBS.

Conflict of Interest: The authors declare no competing financial interest.

Acknowledgment. This work was supported by the National Basic Research Program of China (973 Program, No. 2011CB933600), the Science Fund for Creative Research Groups of NSFC (No. 20921062), the National Natural Science Foundation of China (21105075; 20833006; 21005056; 30971573), and the ``3551 Talent Program'' of the Administrative Committee of East Lake Hi-Tech Development Zone ([2011]137). We are grateful to X.-D. Gao for kindly providing plasmid pFA6a-kanMX6-PGAL1 and helpful discussions, D.-S. Zhao for HRTEM experiments, and S.-P. Liu for qRT-PCR experiments.

Supporting Information Available: Chemicals and reagents; details of the construction of Δ*gsh1*Δ*gsh2*, P_{GAL1}-*GSH1*, P_{GAL1}-*GSH2*, and P_{GAL1}-*GLR1* strains; TEM, HRTEM, and PL characterization of the CdSe QDs isolated from yeast cells; intracellular CdSe QD fluorescence intensity and microscopic images of Δ*gsh1*Δ*gsh2*; growth curves and biosynthetic yield of yeast strains used in this study; effect of growth phase on the biosynthesis of CdSe QDs; measurements of intracellular glutathione contents of WT, P_{GAL1}-*GSH1*, P_{GAL1}-*GSH2*, and P_{GAL1}-*GLR1* cells. This material is available free of charge *via* the Internet at http://pubs.acs.org.

REFERENCES AND NOTES

1. Dabbousi, B. O.; Rodriguez-Viejo, J.; Mikulec, F. V.; Heine, J. R.; Mattoussi, H.; Ober, R.; Jensen, K. F.; Bawendi, M. G. (CdSe) ZnS Core−Shell Quantum Dots: Synthesis and Characterization of a Size Series of Highly Luminescent Nanocrystallites. *J. Phys. Chem. B* **1997**, *101*, 9463–9475.
2. Sun, Y.; Xia, Y. Shape-Controlled Synthesis of Gold and Silver Nanoparticles. *Science* **2002**, *298*, 2176–2179.
3. Pradhan, N.; Peng, X. Efficient and Color-Tunable Mn-Doped ZnSe Nanocrystal Emitters: Control of Optical Performance *via* Greener Synthetic Chemistry. *J. Am. Chem. Soc.* **2007**, *129*, 3339–3347.
4. Michalet, X.; Pinaud, F. F.; Bentolila, L. A.; Tsay, J. M.; Doose, S.; Li, J. J.; Sundaresan, G.; Wu, A. M.; Gambhir, S. S.; Weiss, S. Quantum Dots for Live Cells, *In Vivo* Imaging, and Diagnostics. *Science* **2005**, *307*, 538–544.
5. Medintz, I. L.; Clapp, A. R.; Mattoussi, H.; Goldman, E. R.; Fisher, B.; Mauro, J. M. Self-Assembled Nanoscale Biosensors Based on Quantum Dot FRET Donors. *Nat. Mater.* **2003**, *2*, 630–638.
6. Tsunoyama, H.; Sakurai, H.; Negishi, Y.; Tsukuda, T. Size-Specific Catalytic Activity of Polymer-Stabilized Gold Nanoclusters for Aerobic Alcohol Oxidation in Water. *J. Am. Chem. Soc.* **2005**, *127*, 9374–9375.
7. Nann, T.; Skinner, W. M. Quantum Dots for Electro-optic Devices. *ACS Nano* **2011**, *5*, 5291–5295.
8. Dahl, J. A.; Maddux, B. L. S.; Hutchison, J. E. Toward Greener Nanosynthesis. *Chem. Rev.* **2007**, *107*, 2228–2269.
9. Crookes-Goodson, W. J.; Slocik, J. M.; Naik, R. R. Bio-directed Synthesis and Assembly of Nanomaterials. *Chem. Soc. Rev.* **2008**, *37*, 2403–2412.
10. Dickerson, M. B.; Sandhage, K. H.; Naik, R. R. Protein- and Peptide-Directed Syntheses of Inorganic Materials. *Chem. Rev.* **2008**, *108*, 4935–4978.
11. Mao, C.; Solis, D. J.; Reiss, B. D.; Kottmann, S. T.; Sweeney, R. Y.; Hayhurst, A.; Georgiou, G.; Iverson, B.; Belcher, A. M. Virus-Based Toolkit for the Directed Synthesis of Magnetic and Semiconducting Nanowires. *Science* **2004**, *303*, 213–217.
12. Naik, R. R.; Jones, S. E.; Murray, C. J.; McAuliffe, J. C.; Vaia, R. A.; Stone, M. O. Peptide Templates for Nanoparticle Synthesis Derived from Polymerase Chain Reaction-Driven Phage Display. *Adv. Funct. Mater.* **2004**, *14*, 25–30.
13. Reichhardt, C.; Uchida, M.; O'Neil, A.; Li, R.; Prevelige, P. E.; Douglas, T. Templated Assembly of Organic−Inorganic Materials Using the Core Shell Structure of the P22 Bacteriophage. *Chem. Commun.* **2011**, *47*, 6326–6328.
14. Komeili, A.; Li, Z.; Newman, D. K.; Jensen, G. J. Magnetosomes Are Cell Membrane Invaginations Organized by the Actin-like Protein MamK. *Science* **2006**, *311*, 242–245.
15. Kröger, N.; Deutzmann, R.; Sumper, M. Polycationic Peptides from Diatom Biosilica That Direct Silica Nanosphere Formation. *Science* **1999**, *286*, 1129–1132.
16. Klaus, T.; Joerger, R.; Olsson, E.; Granqvist, C. G. Silver-Based Crystalline Nanoparticles, Microbially Fabricated. *Proc. Natl. Acad. Sci. U.S.A.* **1999**, *96*, 13611–13614.
17. Reith, F.; Etschmann, B.; Grosse, C.; Moors, H.; Benotmane, M. A.; Monsieurs, P.; Grass, G.; Doonan, C.; Vogt, S.; Lai, B.; *et al*. Mechanisms of Gold Biomineralization in the Bacterium *Cupriavidus metallidurans*. *Proc. Natl. Acad. Sci. U.S.A.* **2009**, *106*, 17757–17762.
18. Cui, R.; Liu, H. H.; Xie, H. Y.; Zhang, Z. L.; Yang, Y. R.; Pang, D. W.; Xie, Z. X.; Chen, B. B.; Hu, B.; Shen, P. Living Yeast Cells as a Controllable Biosynthesizer for Fluorescent Quantum Dots. *Adv. Funct. Mater.* **2009**, *19*, 2359–2364.
19. Sweeney, R. Y.; Mao, C.; Gao, X.; Burt, J. L.; Belcher, A. M.; Georgiou, G.; Iverson, B. L. Bacterial Biosynthesis of Cadmium Sulfide Nanocrystals. *Chem. Biol.* **2004**, *11*, 1553–1559.
20. Dameron, C. T.; Reese, R. N.; Mehra, R. K.; Kortan, A. R.; Carroll, P. J.; Steigerwald, M. L.; Brus, L. E.; Winge, D. R. Biosynthesis of Cadmium Sulphide Quantum Semiconductor Crystallites. *Nature* **1989**, *338*, 596–597.
21. Nishida, K.; Silver, P. A. Induction of Biogenic Magnetization and Redox Control by a Component of the Target of Rapamycin Complex 1 Signaling Pathway. *PLoS Biol.* **2012**, *10*, e1001269.
22. Ma, X.; Chen, H.; Yang, L.; Wang, K.; Guo, Y.; Yuan, L. Construction and Potential Applications of a Functionalized Cell with an Intracellular Mineral Scaffold. *Angew. Chem., Int. Ed.* **2011**, *50*, 7414–7417.
23. Kowshik, M.; Vogel, W.; Urban, J.; Kulkarni, S. K.; Paknikar, K. M. Microbial Synthesis of Semiconductor PbS Nanocrystallites. *Adv. Mater.* **2002**, *14*, 815–818.
24. Scheffel, A.; Gruska, M.; Faivre, D.; Linaroudis, A.; Plitzko, J. M.; Schüler, D. An Acidic Protein Aligns Magnetosomes Along a Filamentous Structure in Magnetotactic Bacteria. *Nature* **2006**, *440*, 110–114.
25. Grünberg, K.; Wawer, C.; Tebo, B. M.; Schüler, D. A Large Gene Cluster Encoding Several Magnetosome Proteins Is Conserved in Different Species of Magnetotactic Bacteria. *Appl. Environ. Microbiol.* **2001**, *67*, 4573–4582.
26. Cui, R.; Zhang, M. X.; Tian, Z. Q.; Zhang, Z. L.; Pang, D. W. Intermediate-Dominated Controllable Biomimetic Synthesis of Gold Nanoparticles in a Quasi-Biological System. *Nanoscale* **2010**, *2*, 2120–2125.
27. Zhang, M. X.; Cui, R.; Zhao, J. Y.; Zhang, Z. L.; Pang, D. W. Synthesis of Sub-5 nm Au−Ag Alloy Nanoparticles Using Bio-reducing Agent in Aqueous Solution. *J. Mater. Chem.* **2011**, *21*, 17080–17082.

28. Zhang, M. X.; Cui, R.; Tian, Z. Q.; Zhang, Z. L.; Pang, D. W. Kinetics-Controlled Formation of Gold Clusters Using a Quasi-biological System. *Adv. Funct. Mater.* **2010**, *20*, 3673–3677.
29. Cui, R.; Gu, Y. P.; Zhang, Z. L.; Xie, Z. X.; Tian, Z. Q.; Pang, D. W. Controllable Synthesis of PbSe Nanocubes in Aqueous Phase Using a Quasi-biosystem. *J. Mater. Chem.* **2012**, *22*, 3713–3716.
30. Gu, Y. P.; Cui, R.; Zhang, Z. L.; Xie, Z. X.; Pang, D. W. Ultrasmall Near-Infrared Ag_2Se Quantum Dots with Tunable Fluorescence for *in Vivo* Imaging. *J. Am. Chem. Soc.* **2012**, *134*, 79–82.
31. Dormer, U. H.; Westwater, J.; McLaren, N. F.; Kent, N. A.; Mellor, J.; Jamieson, D. J. Cadmium-Inducible Expression of the Yeast *GSH1* Gene Requires a Functional Sulfur-Amino Acid Regulatory Network. *J. Biol. Chem.* **2000**, *275*, 32611–32616.
32. Pinson, B.; Sagot, I.; Daignan-Fornier, B. Identification of Genes Affecting Selenite Toxicity and Resistance in *Saccharomyces cerevisiae*. *Mol. Microbiol.* **2000**, *36*, 679–687.
33. Eisenstein, M. Bacteria Find Work as Amateur Chemists. *Nat. Methods* **2005**, *2*, 6–7.
34. Giaever, G.; Chu, A. M.; Ni, L.; Connelly, C.; Riles, L.; Véronneau, S.; Dow, S.; Lucau-Danila, A.; Anderson, K.; André, B.; *et al*. Functional Profiling of the *Saccharomyces cerevisiae* Genome. *Nature* **2002**, *418*, 387–391.
35. Longtine, M. S.; McKenzie, A., III; Demarini, D. J.; Shah, N. G.; Wach, A.; Brachat, A.; Philippsen, P.; Pringle, J. R. Additional Modules for Versatile and Economical PCR-Based Gene Deletion and Modification in *Saccharomyces cerevisiae*. *Yeast* **1998**, *14*, 953–961.
36. Wheeler, G. L.; Trotter, E. W.; Dawes, I. W.; Grant, C. M. Coupling of the Transcriptional Regulation of Glutathione Biosynthesis to the Availability of Glutathione and Methionine *via* the Met4 and Yap1 Transcription Factors. *J. Biol. Chem.* **2003**, *278*, 49920–49928.
37. Grant, C. M.; MacIver, F. H.; Dawes, I. W. Glutathione Synthetase Is Dispensable For Growth under Both Normal and Oxidative Stress Conditions in the Yeast *Saccharomyces cerevisiae* Due to an Accumulation of the Dipeptide γ-Glutamylcysteine. *Mol. Biol. Cell* **1997**, *8*, 1699–1707.
38. Grant, C. M. Role of the Glutathione/Glutaredoxin and Thioredoxin Systems in Yeast Growth and Response to Stress Conditions. *Mol. Microbiol.* **2001**, *39*, 533–541.
39. Ohtake, Y.; Yabuuchi, S. Molecular Cloning of the γ-Glutamylcysteine Synthetase Gene of *Saccharomyces cerevisiae*. *Yeast* **1991**, *7*, 953–961.
40. Hietala, K. A.; Lynch, M. L.; Allshouse, J. C.; Johns, C. J.; Roane, T. M. A Mathematical Model of *Saccharomyces cerevisiae* Growth in Response to Cadmium Toxicity. *J. Basic Microbiol.* **2006**, *46*, 196–202.
41. Bronzetti, G.; Cini, M.; Andreoli, E.; Caltavuturo, L.; Panunzio, M.; Croce, C. D. Protective Effects of Vitamins and Selenium Compounds in Yeast. *Mutat. Res.* **2001**, *496*, 105–115.
42. Yu, W. W.; Qu, L.; Guo, W.; Peng, X. Experimental Determination of the Extinction Coefficient of CdTe, CdSe, and CdS Nanocrystals. *Chem. Mater.* **2003**, *15*, 2854–2860.
43. Dernovics, M.; Far, J.; Lobinski, R. Identification of Anionic Selenium Species in Se-Rich Yeast by Electrospray QTOF MS/MS and Hybrid Linear Ion Trap/Orbitrap MS^n. *Metallomics* **2009**, *1*, 317–329.
44. Lee, T. I.; Rinaldi, N. J.; Robert, F.; Odom, D. T.; Bar-Joseph, Z.; Gerber, G. K.; Hannett, N. M.; Harbison, C. T.; Thompson, C. M.; Simon, I.; *et al*. Transcriptional Regulatory Networks in *Saccharomyces cerevisiae*. *Science* **2002**, *298*, 799–804.
45. Xie, H. Y.; Zuo, C.; Liu, Y.; Zhang, Z. L.; Pang, D. W.; Li, X. L.; Gong, J. P.; Dickinson, C.; Zhou, W. Cell-Targeting Multifunctional Nanospheres with Both Fluorescence and Magnetism. *Small* **2005**, *1*, 506–509.
46. Ro, D. K.; Paradise, E. M.; Ouellet, M.; Fisher, K. J.; Newman, K. L.; Ndungu, J. M.; Ho, K. A.; Eachus, R. A.; Ham, T. S.; Kirby, J.; *et al*. Production of the Antimalarial Drug Precursor Artemisinic Acid in Engineered Yeast. *Nature* **2006**, *440*, 940–943.
47. Date, A.; Pasini, P.; Sangal, A.; Daunert, S. Packaging Sensing Cells in Spores for Long-Term Preservation of Sensors: A Tool for Biomedical and Environmental Analysis. *Anal. Chem.* **2010**, *82*, 6098–6103.
48. Simth, P. K.; Krohn, R. I.; Hermanson, G. T.; Mallia, A. K.; Gartner, F. H.; Provenzano, M. D.; Fujimoto, E. K.; Goeke, N. M.; Olson, B. J.; Klenk, D. C. Measurement of Protein Using Bicinchoninic Acid. *Anal. Biochem.* **1985**, *150*, 76–85.
49. Schmitt, M. E.; Brown, T. A.; Trumpower, B. L. A Rapid and Simple Method for Preparation of RNA from *Saccharomyces cerevisiae*. *Nucleic Acids Res.* **1990**, *18*, 3091–3092.
50. Vandesompele, J.; De Preter, K.; Pattyn, F.; Poppe, B.; Van Roy, N.; De Paepe, A.; Speleman, F. Accurate Normalization of Real-Time Quantitative RT-PCR Data by Geometric Averaging of Multiple Internal Control Genes. *Genome Biol.* **2002**, *3*, paper no. RESEARCH0034.
51. Vandeputte, C.; Guizon, I.; Genestie-Denis, I.; Vannier, B.; Lorenzon, G. A Microtiter Plate Assay for Total Glutathione and Glutathione Disulfide Contents in Cultured/Isolated Cells: Performance Study of a New Miniaturized Protocol. *Cell Biol. Toxicol.* **1994**, *10*, 415–421.